Lennard-Jones fluid-fluid interfaces under shear

Guillaume Galliero*

Laboratoire des Fluides Complexes (UMR-5150 with CNRS and TOTAL), Université de Pau et des Pays de l'Adour, BP 1155, 64013 Pau Cedex, France

(Received 26 October 2009; revised manuscript received 9 March 2010; published 6 May 2010)

Using nonequilibrium molecular dynamics simulations on simple Lennard-Jones binary mixtures, we have studied the behavior of planar fluid-fluid interfaces undergoing shear flow. When the miscibility is low enough, a slip together with a partial depletion have been noticed at the interface between the two fluid phases. The slip length can reach a value equal to some molecular diameters and the corresponding interfacial viscosity can be two times smaller than the value in the bulk. It is shown how the omission of this slip may lead to flow-rate misevaluation when dealing with a multiphase flow in a nanoporous medium even for non polymer fluids. In addition, using the simulation results, a simple relation between interfacial tension and interfacial viscosity is proposed for the monoatomic systems studied in this work. Finally, it is shown that the interfacial viscosity cannot be fully accounted for by estimating the local viscosity deduced from the local thermodynamic properties of the interface.

DOI: 10.1103/PhysRevE.81.056306 PACS number(s): 47.61.Jd, 47.11.Mn, 66.20.−d, 83.50.Lh

I. INTRODUCTION

With the increased interest in micro/nanofluidics and microelectromechanical devices [1,2], a great effort has been dedicated to the improvement of the understanding of the heat and mass transfers at the atomic scale along and across interfaces [1–8]. In particular, many works have been dedicated to the estimation of the slip of simple Newtonian fluids at the fluid-solid interface in the nondilute regime [1,7,8]. However, it is not always easy to analyze experimental results in Newtonian liquids because of the various parameters that may affect the slip [8]. A way to study well controlled systems is to employ molecular dynamics (MD) simulation on given fluid models in contact with an idealized solid surface of a chosen geometry. In particular, thanks to molecular dynamics simulation on model liquid confined in nanopores, it has been shown that a non negligible slip can occur at a fluid-solid interface (non wetting and perfectly flat at the atomic scale) even for a monoatomic fluid [9,10]. Rather surprisingly, there is far less studies of fluid-fluid interfaces under shear and most of them deal with polymer systems [11–17].

From a macroscopic point of view, it is still generally assumed that, at a fluid-fluid interface there is both equality of the tangential velocities and equality of the shear stress [18], except in polymer science where a partial/apparent slip is sometimes accounted for [13–15]. In fact, there are some experimental evidences of such polymer-polymer apparent interfacial slip [15] which is usually consistent with theories [11,13] and which has been noticed as well by MD simulations [12,14]. Generally, this apparent slip is related to the peculiar behavior (conformation, entanglement) of the chains at the interface which induces an interfacial viscosity lower than the one in the bulk regions [13,15]. However, Padilla *et al.* [12] and latter Koplik and Banavar [14] have shown that, even in monoatomic fluids, a partial slip can appear at a liquid-liquid interface between two immiscible fluids using MD simulations. Nevertheless, they do not provide a full explanation of this slip in systems, which are not composed of chainlike molecules.

So, to improve the analysis of the momentum transfer across simple fluid-fluid (composed of monoatomic species) interfaces and to study and quantify a possible slip, we have performed nonequilibrium molecular dynamics (NEMD) simulations of planar fluid-fluid interfaces undergoing a shear flow. The systems simulated are composed of two species possessing the same molecular parameters. They are described by Lennard-Jones spheres for which cross interactions have been modulated to change the miscibility between the compounds. Then, using the NEMD results, a possible link between equilibrium and non equilibrium properties is discussed together with an analysis of the interfacial viscosity in the frame of a local viscosity depending on the local thermodynamic properties.

II. MODELS

A. System studied

The two-phase systems studied in this work are composed of binary equimolar mixtures of simple spherical particles. Interactions are described by a usual truncated Lennard-Jones (LJ) 12–6 potential,

$$U_{ij}=\begin{cases}4\varepsilon_{ij}\left[\left(\dfrac{\sigma_{ij}}{r_{ij}}\right)^{12}-\left(\dfrac{\sigma_{ij}}{r_{ij}}\right)^{6}\right] & \text{if } r_{ij}\le r_c\\ 0 & \text{if } r_{ij}>r_c,\end{cases} \tag{1}$$

where r_{ij} is the distance between particles i and j, ε is the potential depth, σ is the particle "diameter," and r_c the cutoff radius ($=3.5\sigma$ in this work).

To reduce the complexity of the systems studied, the molecular parameters of the two species have been taken equal, i.e., $\sigma_{11}=\sigma_{22}=\sigma$, $\varepsilon_{11}=\varepsilon_{22}=\varepsilon$, and $m_1=m_2=m$, where m_i is the molecular mass of component i. Then, to modulate the miscibility between the two species, the cross interactions

*FAX: +33 5 59 40 7695; guillaume.galliero@univ-pau.fr

 ©2010 The American Physical Society

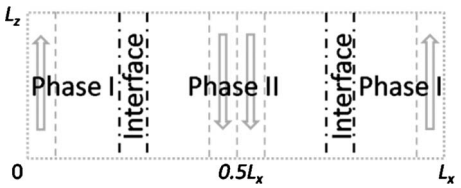

FIG. 1. A 2D (x,z) sketch of the simulation box containing the two-phases and the fluid-fluid interfaces sheared biperiodically (with full periodic boundary conditions).

between the two components have been changed by using a classical k_{ij} prefactor,

$$\varepsilon_{12} = k_{ij}\varepsilon. \tag{2}$$

By doing so, when k_{ij} is small enough (in our case below ~ 0.8) this ensures that the excess of direct attractive interactions (i.e., between species 1–1 and 2–2) relatively to the cross interactions (between unlike species 1–2) is sufficient to overcome the tendency to mix due to entropy [19]. In the following all quantities are provided in LJ dimensionless units (using σ, ε, and m) and noted with a star as superscript.

To build the initial configuration of the simulation box, particles from species 1 are randomly distributed between 0 and $L_x/4$, where L_x is the length of the simulation box along x, and between $3L_x/4$ and L_x, and particles from species 2 are placed between $L_x/4$ and $3L_x/4$. Then, an equilibrium molecular dynamics (with full periodic boundary conditions) simulation is performed to reach the two-phase equilibrium state.

When k_{ij} is small enough to induce non/weak miscibility, this initialization ensures a biperiodical two-phase (phases I and II) configuration along the x direction because of the symmetry of the system studied around $L_x/2$, see Fig. 1. This symmetry is due to the fact that the two phases so constructed are completely equivalent because of the molecular properties of the two species $\sigma_{11}=\sigma_{22}$ and $\varepsilon_{11}=\varepsilon_{22}$. By convention, we will note phase I, the phase in which species 1 is more concentrated than species 2.

After equilibration the two planar interfaces between phases I and II are located around $L_x/4$ and $3L_x/4$, see Fig. 1. It is worth to mention that the dimensions of the system have been chosen so that the distance between the two interfaces is larger than two times the cut-off radius. This ensures that no interactions occur between the two interfaces.

B. NEMD scheme

To shear the two-phase system so constructed, we have employed a NEMD scheme derived from the one proposed by F. Müller-Plathe [20], which was developed to compute shear viscosity efficiently. First, the simulation box is divided into N_s slabs (40 in this work) along the x direction. Then, the fluid is sheared, see Fig. 1, using a net exchange of the linear momentum along the direction z, Δp_z, which is performed between the central part of the simulation box, $N_s/2$ and $N_s/2+1$ (center of phase II), and the edge layers, slab 1 and N_s (center of phase I). To do so, we simply add $\Delta p_z/2$ to the particles located in slabs 1 and N_s and we withdraw the same amount of momentum to the particles located in slabs $N_s/2$ and $N_s/2+1$ at each time step. At the stationary state, this NEMD scheme induces a biperiodical velocity profile in the simulation box.

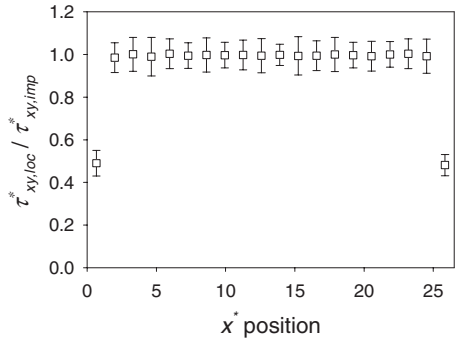

FIG. 2. Local shear stress, relatively to the imposed value, over half of the simulation box for $k_{ij}=0.25$ at $T^*=1$. The fluid-fluid interface is located approximately between $x^*\approx 10$ and $x^*\approx 15$.

To avoid shear thinning, we have tested various values of Δp_z. It has been found that a good signal to noise ratio in the linear response regime, can be obtained by using a value of Δp_z^* corresponding to an imposed shear stress (transverse linear momentum flux) $\tau^*_{xz,\mathrm{imp}}=0.05$. This shear stress value is below the shear thinning threshold of the pure LJ fluid [21].

In addition, to verify that the shear stress was not affected by the presence of the fluid-fluid interface, both the classical Irving-Kirkwood and the method of plane microscopic formulations have been used [22] to estimate the local shear stress $\tau^*_{xz,\mathrm{loc}}$. As confirmed on Fig. 2, the computed local shear stress is equal to the imposed one even across the interface. However, because of the biperiodical NEMD scheme employed, the local shear stress is different from the imposed one in the regions where the momentum exchange is performed. So, the slabs where the momentum exchange is performed, as well as their first neighbors, have been discarded for the analysis of the results. Besides, by computing the local temperature, it has been checked that the shear stress employed was sufficiently small to have a negligible impact on the temperature profile.

C. Numerical details

To perform the simulations, a homemade code already validated on one and two-phase systems has been employed [23,24]. In all cases simulations have been performed using 2000 LJ particles of each species. The Verlet velocity algorithm has been used to integrate the motion's equation with a reduced time step of $\delta t^*=0.003$. Full periodic boundary conditions combined with a Verlet neighbors list have been applied. To maintain constant the average temperature during the simulations, a Berendsen thermostat has been used on the x and y components of the velocity [25].

To estimate local quantities, the simulation box has been divided into 200 slabs along the direction x, which is sufficient to obtain results that are independent of the number of slabs. To perform the analysis in the following, results have

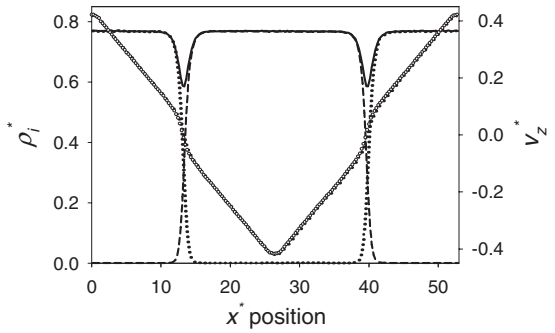

FIG. 3. Density (full line: ρ^*, dotted line: ρ_1^*, dashed line: ρ_2^*) and velocity (circles: v_z^*) profiles of the sheared two-phase system at the stationary state for $k_{ij}=0.25$ at $T^*=1$.

been averaged over the two half simulation boxes (along x) taking advantage of the symmetry of the system studied, see Fig. 1. Equilibrium properties have been estimated using runs of 2×10^6 time steps. For non equilibrium properties, they have been computed using runs of at least 5×10^6 time steps during the stationary state. In order to estimate errors on the computed variables, the sub-blocks average method has been applied [26].

III. RESULTS

A. Equilibrium properties

First, a set of equilibrium MD simulations have been performed at a fixed temperature, $T^*=1$, and a given average density, $\rho^*=0.7547$ (a liquid state for a pure LJ fluid). To modify the interfacial properties, we have employed different k_{ij} ranging from 0.125 to 0.75 with a step of 0.125, the lower the k_{ij} the lower the miscibility between the compounds. An example of density profiles obtained after equilibration is shown on Fig. 3. It is worth to mention that there is a noticeable depleted region (zone of total density lower than in the bulk) between the two phases as found in Refs. [4,12,17], see Fig. 3.

To define a degree of mixing of the two species for the different k_{ij} used, we have computed in the bulk region an equilibrium constant K defined as

$$K=\frac{x_{1,II}}{x_{1,I}}, \tag{3}$$

where $x_{1,I}$ is the molar fraction of species 1 in phase I and $x_{1,II}$ the molar fraction of species 1 in phase II (for the systems studied here, we have always $x_{1,I}\geq x_{1,II}$). Such a definition implies that $K=0$ when the two species are fully immiscible and $K=1$ when the two species are fully miscible.

To quantify the amplitude of the depletion at the interface, we have estimated a relative depletion, δ, defined by

$$\delta=\frac{\rho_{\min}^*}{\rho_{\text{bulk}}^*}, \tag{4}$$

where $\rho_{\min}^*$ is the minimum value of the density profile (located at the interface, see Fig. 3) and ρ_{bulk}^* is the average density of the bulk region.

In order to determine the interfacial tension, γ^*, between the two phases, the classical mechanic route has been employed [27], i.e., the interfacial tension has been determined from:

$$\gamma^*=\frac{1}{2}\int_0^{L_x^*}[P_N^*(x^*)-P_T^*(x^*)]dx^*, \tag{5}$$

where $P_N^*(x^*)$ and $P_T^*(x^*)$ are, respectively, the normal and tangential components (relatively to the interface) of the pressure at the position x^*.

The interfacial width, L_{int}, has been estimated from the density profiles of the two compounds, ρ_1 and ρ_2. More precisely, we have defined L_{int} as the distance between the x position where ρ_1 becomes smaller than 99% of its bulk value and the x position where ρ_2 becomes bigger than 99% of its bulk value. Such a definition of the interface width has been chosen in order to avoid the need to choose an analytical form to describe the density profiles [27].

As shown in Table I, in all cases studied here even with $k_{ij}=0.125$, the two species are not fully immiscible, i.e., $K>0$, the concentration of species 1 (and 2) is everywhere not equal to zero. As expected, both K and δ increases with k_{ij}. Furthermore the mixing between the species remains generally small (i.e., $K<5\%$) except when $k_{ij}=0.75$ which is a value very close to the miscibility threshold.

Concerning the depletion at the interface, it remains rather limited compared to the ones obtained other studies [12,17]. This is probably due to the fact that they [12,17] employ purely repulsive interactions between unlike pairs whereas we employ a classical Lennard-Jones potential with attractive interactions between unlike particles, Eq. (1). In addition, it is interesting to note that δ depends nearly linearly on k_{ij}, see Table I.

The interfacial tension, γ^*, decreases noticeably with the increase in k_{ij}. This is consistent with what can be expected on simple systems [27]. In addition, it is interesting to point out that the amplitude of γ^* for the lowest values of k_{ij} is

TABLE I. Equilibrium interfacial properties (equilibrium constant, K, relative depletion, δ, interfacial tension, γ^*, and width, L_{int}^*) for different values of cross interactions amplitude, k_{ij}.

k_{ij}	0.125	0.25	0.375	0.5	0.625	0.75
K (in %)	0.13 ± 0.02	0.17 ± 0.02	0.41 ± 0.06	1.11 ± 0.19	4.08 ± 0.55	32 ± 3.1
δ	0.725 ± 0.005	0.763 ± 0.004	0.819 ± 0.009	0.873 ± 0.004	0.931 ± 0.007	0.988 ± 0.004
γ^*	1.54 ± 0.04	1.33 ± 0.04	1.08 ± 0.05	0.78 ± 0.03	0.43 ± 0.05	0.09 ± 0.07
L_{int}^*	5.3 ± 0.2	5.2 ± 0.2	5.3 ± 0.3	5.6 ± 0.3	6.5 ± 0.3	12.5 ± 2.4

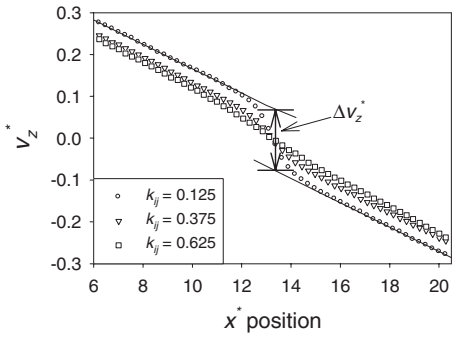

FIG. 4. Velocity profiles across the interface at the stationary state for various k_{ij}. Full tangent lines allow to estimate the velocity jump, Δv_z^*, at the interface.

rather important for a non polar system, see Table I; for a LJ liquid-vapor interface at a temperature close to that of the triple point, γ^* is approximately equal to 1.1 [28]. Concerning L_{int}^*, it remains nearly constant up to k_{ij}=0.375 and then increases with the increase in k_{ij}, see Table I.

B. Nonequilibrium properties

In a second step, for the same conditions than in the previous section, NEMD simulations have been performed. First, it has been verified that K, δ, L_{int}^*, and γ^* deduced from NEMD simulations were consistent with the values obtained during equilibrium simulations. In all cases NEMD results have been found to be within the error bars of those deduced from equilibrium simulations as expected for low enough shear stress [29] and similarly to what found when a temperature gradient is applied perpendicularly to an interface [3].

More important is the obvious slip which appears between the two fluid phases for sufficiently low values of k_{ij} as clearly shown on Figs. 3 and 4. From a macroscopic point of view, this slip can be interpreted as due to a local decrease of the apparent viscosity in the interface, an interfacial viscosity with a value lower than in the two phases [13,14]. In other words, the interface introduces a resistance to the linear momentum transfer as it is the case for thermal transfer [3] as well.

In polymer science, such a result is well known [11,13–17] and has been studied using NEMD simulations on model polymer [14,16,17] but less is known and understood concerning the monoatomic fluids cases [12,17]. The explanation of the reduction of the viscosity in the interface is often related to an effect due to the modification of the configuration and entanglement of the chains at the interface [13,14]. In the case studied in this work the systems are monoatomic and so such an explanation cannot hold.

To quantify the slip, we have measured the velocity jump, Δv_z, induced by the presence of the interface. To do so, the velocity profiles of the phases in the bulk regions have been extrapolated linearly to the center of the interface as shown for k_{ij}=0.125 on Fig. 4. Then, Δv_z has been estimated from the difference between the extrapolated velocities of each phases, see Fig. 4. Next, by considering a Navier boundary condition [1] (at the interface) the slip coefficient/length, α, can be deduced from the velocity jump at the interface using:

$$\alpha^* = \frac{\Delta v_z^*}{\tau_{xz}^*}. \tag{6}$$

In addition, we have defined the interfacial viscosity, η_{int}^*, as the apparent viscosity of the interface over the interfacial width, L_{int}^* defined previously. Using that definition we can define the interfacial viscosity as:

$$\eta_{\text{int}}^* = \frac{\tau_{xz}^* L_{\text{int}}^*}{\Delta v_{z,\text{int}}^*} \tag{7}$$

where $\Delta v_{z,\text{int}}^*$ is the variation of the velocity over the interfacial width. In addition, $\Delta v_{z,\text{int}}^*$ is simply the sum of the velocity jump Δv_z^* and the velocity difference over L_{int}^* without the velocity jump, i.e.,:

$$\Delta v_{z,\text{int}}^* = \Delta v_z^* + \frac{\tau_{xz}^* L_{\text{int}}^*}{\eta_{\text{bulk}}^*}, \tag{8}$$

where η_{bulk}^* is the viscosity of the bulk region computed during the NEMD simulations for each k_{ij}. So, by combining Eqs. (7) and (8) we can deduce that

$$\eta_{\text{int}}^* = \frac{\tau_{xz}^* L_{\text{int}}^* \eta_{\text{bulk}}^*}{\tau_{xz}^* L_{\text{int}}^* + \Delta v_z^* \eta_{\text{bulk}}^*}. \tag{9}$$

All α^*, η_{bulk}^*, and η_{int}^* values obtained for each k_{ij} are provided in Table II.

As expected, α^* increases and η_{int}^* decreases monotonically when k_{ij} decreases, i.e., when the interfacial tension between the fluid increases. The slip length, α^*, can be non negligible as it can reach roughly 3 molecular diameters, i.e., $\sim$1 nm for an argon type fluid. This value is rather small compared to what can occur at fluid-solid interface (nonwetting and perfectly flat at the atomic scale), for which α^* can exceed 30 [9]. However the slip at a fluid-solid interface is generally reduced if the solid surface is rough [30], whereas at a fluid-fluid interface, the interface will be always "roughless," except in the presence of impurities at the interface.

TABLE II. Nonequilibrium interfacial properties (slip length, α^*, bulk viscosity, η_{bulk}^*, and interfacial viscosity, η_{int}^*) for different values of cross interactions amplitude, k_{ij}.

k_{ij}	0.125	0.25	0.375	0.5	0.625	0.75
α^*	2.96 ± 0.18	2.12 ± 0.12	1.56 ± 0.12	1.1 ± 0.18	0.68 ± 0.1	0.19 ± 0.11
η_{bulk}^*	1.73 ± 0.14	1.72 ± 0.13	1.69 ± 0.14	1.66 ± 0.15	1.6 ± 0.17	1.55 ± 0.13
η_{int}^*	0.88 ± 0.15	1.01 ± 0.17	1.13 ± 0.2	1.25 ± 0.25	1.37 ± 0.21	1.51 ± 0.14

Concerning the interfacial viscosity, its amplitude can be largely smaller than its corresponding bulk value, e.g., for $k_{ij}=0.125$, η^*_{int} is two times smaller than η^*_{bulk} see Table II. This result is important as it implies that the global apparent viscosity of a two-phase system can be largely smaller than the one deduced only from the viscosity of the two phases as long as the width of the interface is not negligible compared to the size of the global system. More precisely, in a two-phase system (planar) sheared parallel to the interface, the apparent viscosity, η_{app}, is given by

$$\frac{L_1+L_2}{\eta_{\mathrm{app}}}=\frac{L_1}{\eta_1}+\frac{L_2}{\eta_2}, \tag{10}$$

where L_i and η_i are, respectively, the width and the viscosity of phase i. However, if we take into account the interfacial region, the correct apparent viscosity, $\eta^{\mathrm{int}}_{\mathrm{app}}$, which is smaller than η_{app}, would be given by

$$\frac{L_1+L_{\mathrm{int}}+L_2}{\eta^{\mathrm{int}}_{\mathrm{app}}}=\frac{L_1}{\eta_1}+\frac{L_{\mathrm{int}}}{\eta_{\mathrm{int}}}+\frac{L_2}{\eta_2}. \tag{11}$$

To give an order of magnitude of the impact of this partial slip on a multiphase flow in a nanopore, we consider an ideal slit pore (with ideal no slip conditions at the fluid-solid interfaces) filled by two phases, one fully wetting and the second one nonwetting and nonmiscible with the first phase which implies two planar interfaces between phases I and phase II. For the fluids properties we consider the two-phase system studied in this work for $k_{ij}=0.125$ (corresponding to $L^*_{\mathrm{int}}\approx 5$ and $\eta^*_{\mathrm{int}}\approx \eta^*_{\mathrm{bulk}}/2$, see Table II) and for the pore a width $D^*=30$. In addition, both the width of phase 2 and the sum of the widths of the two parts of phase 1 are chosen to be equal to $L^*=10$. For that configuration using Eq. (11), we get $\frac{\eta^{\mathrm{int}}_{\mathrm{app}}}{\eta_{\mathrm{bulk}}}=\frac{3}{4}$.

Thus, for that peculiar system, the value of the flow-rate taking into account the slip between the fluid phases is approximately 33% higher than the one when omitting the slip at the fluid-fluid interfaces. For simple argonlike fluid, such a configuration corresponds to a pore width of the order of 10^{-8} m, which corresponds to an absolute permeability of the order of 0.01 mDa. It is worth to notice that, by taking into account a slip between the nonmiscible fluid phases implies that one considers that the relative permeabilities [31] are a function of the pore size when dealing with multiphase flow in low permeability systems.

C. Interfacial viscosity

In a first approximation to relate the interfacial viscosity to other properties, one can assume a simple link between the interfacial viscosity and the interfacial tension. Such a link is intuitively understandable as long as increasing the interfacial tension will necessarily disfavors the momentum transfer from one phase to another. For the systems studied in this work we have found that the relation,

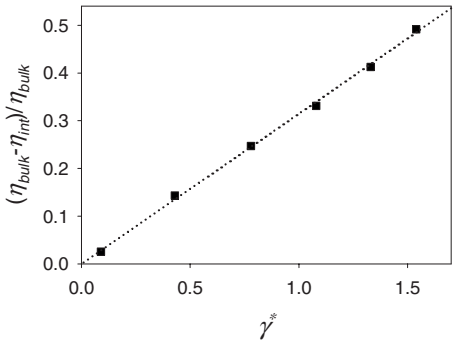

FIG. 5. Behavior of the interfacial viscosity with the interfacial tension for all k_{ij}. The squares correspond to the NEMD results and the dotted line to Eq. (12).

$$\frac{\eta^*_{\mathrm{bulk}}-\eta^*_{\mathrm{int}}}{\eta^*_{\mathrm{bulk}}}=a\gamma^*, \tag{12}$$

where a is a constant (=0.315 in this case), holds for all k_{ij} see Fig. 5. This simple relation, even if tested only for the system studied in this work, indicates that for monoatomic systems the interfacial viscosity is probably mainly modulated by thermodynamic effects and not by kinetic ones. This is not surprising as long as the amplitude of the LJ viscosity in dense phases (as in this work) is only weakly due to the kinetic contribution [21].

Another simple picture to explain the low η^*_{int} values compared to η^*_{bulk} ones is to assume that this effect is due to the local thermodynamic conditions (depletion) at the interface. To test that assumption, we have estimated the local viscosity in each slab from the local temperature, density and composition, even if the concept of local viscosity at such scale is largely questionable [32]. To do so, as direct simulations are not possible in the unstable regions, i.e., in the interface, we have employed an accurate empirical correlation [23] to estimate the viscosity in the bulk and the interface regions from their thermodynamic properties (temperature, density and composition).

This empirical correlation has been fitted on a large MD database [23] and is able to provide the viscosity of the LJ pure fluid with an error below 5% compared to MD simulations results whatever the fluid state [23], with density and temperature as inputs. In order to take into account the composition effect, we have combined this correlation with a classical van der Waals one-fluid approximation. Such a scheme is very efficient for LJ mixtures composed of species with similar masses and sizes [33] as are the systems studied in this work. Thus, using the local values of the temperature, density and composition, we have deduced from this correlation the bulk and interface viscosities, respectively $\eta^{\mathrm{corr}}_{\mathrm{bulk}}$ and $\eta^{\mathrm{corr}}_{\mathrm{int}}$.

Using that approach, the bulk viscosity estimated from the correlation and the local thermodynamic properties is always within 2% (i.e., within the error bars) of the value computed directly from the NEMD local velocity field, see Tables II and III. This result confirms the efficiency of the correlation to estimate the viscosity of the systems studied in this work.

TABLE III. Bulk and interfacial viscosities deduced from a viscosity correlation and the local temperature, density and composition profiles.

k_{ij}	0.125	0.25	0.375	0.5	0.625	0.75
$\eta_{\text{bulk}}^{\text{corr}^*}$	1.71	1.7	1.67	1.65	1.62	1.57
$\eta_{\text{int}}^{\text{corr}^*}$	1.15	1.18	1.25	1.33	1.42	1.54

More important is that the interface viscosity deduced from the correlation over the interface width, $\eta_{\text{int}}^{\text{corr}}$, provides a reasonable estimation of the one deduced from the NEMD simulations, η_{int}. However the $\eta_{\text{int}}^{\text{corr}}$ value is always noticeably larger than the η_{int} one, see Tables II and III. The relative differences between these two viscosities are about 31, 16, 10, 6, 4, and 3 percents for, respectively, k_{ij}=0.125, 0.25, 0.375, 0.5, 0.625, and 0.75. This clearly indicates that the interface viscosity that we have deduced directly from NEMD results cannot be fully quantified only by the estimation of a local viscosity deduced from the local thermodynamic conditions. This is not surprising as long as we can suspect that non-local effects have to be taken into account [32] as it is usually done when dealing with interfaces from a thermodynamic point of view, such as done in the gradient theory approach [27,28].

IV. CONCLUSIONS

In this work, we have studied simple fully symmetric fluid-fluid interfaces undergoing shear flow using nonequilibrium molecular dynamics simulations. Interestingly, it has been noticed that, in the interface where a partial depletion appears, the tangential velocity varies more rapidly than in the bulk regions. This indicates that a partial slip exists between two non- (or weakly) miscible fluid phases, even if the system is composed of simple monoatomic LJ particles. In fact, the fluid-fluid interface acts as a resistance to the momentum transfer.

As expected, the slip and the depletion at the interface are decreasing when the miscibility between the two species increases. The slip length can reach 3 molecular diameters and the corresponding interfacial viscosity can be two times smaller than in the bulk. It is important to point out that such an effect can noticeably affect the expected flow-rate when dealing with multiphase flow in low-permeability porous medium.

Using the molecular dynamics results, it has been found that the interfacial viscosity (relatively to its bulk value) can be linearly related to the interfacial tension for the systems studied in this work. In addition, it has been shown that the interfacial viscosity obtained during NEMD simulations cannot be fully accounted for by simply estimating the local viscosity deduced from the local temperature, density and composition at the interface.

ACKNOWLEDGMENTS

This work has been supported by the "Failflow" program of the ERC, the TGR project managed by TOTAL and a program of the *Région Aquitaine*. We acknowledge D. Broseta, M. Bugel, and J.-P. Caltagirone for fruitful discussions.

[1] G. Karniadis, A. Beskok, and N. Aluru, *Microflows and Nanoflows* (Springer, New York, 2005).
[2] B. Y. Cao, J. Sun, M. Chen, and Z. Y. Guo, Int. J. Mol. Sci. **10**, 4638 (2009).
[3] S. Kjelstrup and D. Bedeaux, *Non-Equilibrium Thermodynamics of Heterogeneous Systems* (World Scientific, Singapore, 2008).
[4] M. Meyer, M. Mareschal, and M. Hayoun, J. Chem. Phys. **89**, 1067 (1988).
[5] I. Benjamin, Annu. Rev. Phys. Chem. **48**, 407 (1997).
[6] J. Buhn, P. A. Bopp, and M. J. Hampe, J. Mol. Liq. **125**, 187 (2006).
[7] L. Bocquet and J. L. Barrat, Soft Matter **3**, 685 (2007).
[8] C. Neto, D. R. Evans, E. Bonaccurso, J. H. Butt, and V. S. J. Craig, Rep. Prog. Phys. **68**, 2859 (2005).
[9] J. L. Barrat and L. Bocquet, Faraday Discuss. **112**, 119 (1999).
[10] M. Cieplak, J. Koplik, and J. R. Banavar, Phys. Rev. Lett. **86**, 803 (2001).
[11] F. Brochard-Wyart, P. G. de Gennes, and S. Troian, C. R. Acad Sci., Ser. II: Mec., Phys., Chim., Sci. Terre Univers **310**, 1169 (1990).
[12] P. Padilla, S. Toxvaerd, and J. Stecki, J. Chem. Phys. **103**, 716 (1995).
[13] J. L. Goveas and G. H. Fredrickson, Eur. Phys. J. B **2**, 79 (1998).
[14] S. Barsky and M. O. Robbins, Phys. Rev. E **63**, 021801 (2001).
[15] R. Zhao and C. W. Macosko, J. Rheol. **46**, 145 (2002).
[16] T. S. Lo, M. Mihajlovic, Y. Shnidman, W. Li, and D. Gersappe, Phys. Rev. E **72**, 040801(R) (2005).
[17] J. Koplik and J. R. Banavar, Phys. Rev. Lett. **96**, 044505 (2006).
[18] R. B. Bird, W. E. Stewart, and E. N. Lightfoot, *Transport Phenomena* (Wiley, New York, 2006).
[19] J. Stecki and S. Toxvaerd, J. Chem. Phys. **103**, 4352 (1995).
[20] F. Müller-Plathe, Phys. Rev. E **59**, 4894 (1999).
[21] G. Galliero and C. Boned, Phys. Rev. E **79**, 021201 (2009).
[22] B. D. Todd, D. J. Evans, and P. J. Daivis, Phys. Rev. E **52**, 1627 (1995).
[23] G. Galliero, C. Boned, and A. Baylaucq, Ind. Eng. Chem. Res.

44, 6963 (2005).
[24] G. Galliero and C. Boned, J. Chem. Phys. **129**, 074506 (2008).
[25] H. J. C. Berendsen, *Simulating the Physical World* (Cambridge, Cambridge, England, 2007).
[26] M. P. Allen and D. J. Tildesley, *Computer Simulations of Liquids* (Oxford Science Publications, Oxford, 1987).
[27] J. S. Rowlinson and B. Widom, *Molecular Theory of Capillarity* (Dover, New York, 1982).
[28] G. Galliero, M. M. Piñeiro, B. Mendiboure, C. Miqueu, T. Lafitte, and D. Bessières, J. Chem. Phys. **130**, 104704 (2009).
[29] K. Rah and B. C. Eu, Physica A **292**, 102 (2001).
[30] A. Niavarani and N. V. Priezjev, Phys. Rev. E **81**, 011606 (2010).
[31] J. Bear, *Dynamics of Fluids in Porous Media* (Dover, New York, 1988).
[32] B. D. Todd, J. S. Hansen, and P. J. Daivis, Phys. Rev. Lett. **100**, 195901 (2008).
[33] G. Galliero, C. Boned, A. Baylaucq, and F. Montel, Fluid Phase Equilib. **245**, 20 (2006).